Journal of Nonlinear Modeling and Analysis
Volume 7, Number 6, December 2025, 2314–2329
https://journal.global-sci.org/jnma
DOI:10.12150/jnma.2025.2314

Fractional Order Solution to Analyze Tumor-Immune Cells by Using Hybrid Natural Transform Method and Residual Power Series Method*

Ashrita Patra[1] and Tapasi Pasayat[1,†]

Abstract The purpose of this study is to examine the impact of fractional-order chemotherapy drug diffusion on tumor-immune cell growth. To address the proposed system of fractional-order tumor-immune cell dynamics, two distinct and robust methods have been employed. Initially, the Hybrid Natural Decomposition method, an analytical approach that merges two effective techniques – Natural Transform and the Adomian Decomposition Method has been applied. Subsequently, the Residual Power Series method, a numerical technique, has been employed to derive the solution in series form. The graphical comparison of the results obtained from both methods with those from classical-order solutions has been provided. The findings clearly demonstrate that the proposed approaches offer a reliable and accurate means of understanding the intricate interactions between tumor growth and immune cell activity.

Keywords Chemotherapy, cancer, Residual Power Series method, Natural Transform method, tumor immune cell, fractional derivative, Adomian polynomials

MSC(2010) 26A33, 33C60, 40C05.

1. Introduction

The current challenge of cancer, in terms of sickness and mortality, remains one of the most crucial matters in modern medicine. Despite notable advancements in both fields, the intricacy of tumor development and the complex interplay between cancer cells and the immune system continue to manifest significant obstacles in cancer research and treatment [19, 21]. The emerging field of tumor-immune surveillance has recently drawn surging attention due to its unique perspective on the body's natural defenses against cancer growth [2]. The exact cause of most tumors remaining unknown, specific risk factors like exposure to radiation, tobacco usage, and genetic mutations have been linked to their development [23]. The interaction between tumor cells and immune cells, such as cytotoxic T-cells (CD8+ T cells),

†the corresponding author.
Email address: ashrita.patra@gmail.com, tapashya.94@gmail.com
[1]School of Mathematics, Gangadhar Meher University, Amruta Vihar, Sambalpur, India.
*Funding–This research work was financially supported by OURIIP with grant no.–OURIIP SEED fund–2022/074–Mathematics, dated–10-02-2023.

natural killer (NK) cells, and drug cells, is a multifaceted and dynamic process that plays a critical role in the progression of cancer and the response to treatment. CD8+ T lymphocytes, also referred to as cytotoxic T cells, play a crucial role in the adaptive immune system. They have the ability to identify and remove tumor cells that exhibit particular antigens on their surfaces. This recognition process takes place through antigen presentation, during which tumor cells present tumor-specific antigens on their surface in association with major histocompatibility complex class I (MHC-I) molecules.

Based on prior studies [7, 22], equation (1.1) depicts the fractional order relationship between tumor cells and the anti-tumor immune system, as well as the impact of chemotherapy on both the tumor cells and the immune system in caputo sense.

$$\begin{aligned}
{}^{C}D_t^{\varkappa} N(t) &= \left(\phi N(1-\lambda N) - \mu_1 NT - \delta_1 UN\right), \\
{}^{C}D_t^{\varkappa} L(t) &= \left(\alpha NT - \beta L - \eta_1 LT - \delta_2 UL\right), \\
{}^{C}D_t^{\varkappa} T(t) &= \left(\sigma T(1-\tau T) - \mu_2 NT - \eta_2 LT - \delta_3 UT\right), \\
{}^{C}D_t^{\varkappa} U(t) &= \left(\xi - rU\right).
\end{aligned} \tag{1.1}$$

The research affirms that the model explains how tumor cell and immune system population change under chemotherapy. T represents the population of tumor cells at time t, while N and L respectively represent the population of Natural-Killer cells and cytotoxic T-cells, and U represents the amount of drug at the tumor site. According to the model, the decrease in tumor population is caused by both immune effector cells and chemotherapy. This decrease is a result of the degradation process, which involves the consumption that occurs when tumor cells are killed due to chemotherapy, leading to a subsequent decrease in the population of effector cells. In addition, because chemotherapy drugs impact both tumor cells and immune effector cells using a mass-action mechanism, administering a higher constant dosage of the drug can lead to increased depletion of both the tumor and immune effector cells. The description and values of the parameters used in Eq.(1.1) as per the existing literature [7, 22] are given in Table 1.

By combining the two powerful techniques, Natural Transform(NT) and Adomian Decomposition Method(ADM), the technique Hybrid Natural Decomposition Method(HNDM), offers a unique solution to the complex dynamics of tumor-immune cell interactions, which has not been extensively explored in the existing literature. The HNDM integrates the strengths of NT and ADM, providing an analytical framework that is both efficient and precise for tackling fractional-order differential equations. This allows for a deeper understanding of tumor growth and immune response at fractional orders, a dimension that conventional integer-order models fail to capture.

In addition, the application of the Residual Power Series(RPS) method offers an effective numerical technique to obtain solutions in series form. The use of these methods introduces a new paradigm for solving fractional-order models, enabling a more accurate representation of the dynamic and nonlinear processes governing tumor-immune interactions. These novel approaches not only enhances the precision of predictions in cancer research but also provides valuable insights into the complex relationships among chemotherapy drug diffusion, tumor growth and immune cell responses, opening new avenues for improving cancer treatment strategies.

Table 1. Parameters, Descriptions, and their Values.

Parameter	Description	Value
φ	Growth rate of NK cells	0.25/cell/day
δ_2	CTL cell killed by drug	6×10^{-1}/cell/day
λ	Inverse of NK cells capacity	3.17×10^{-6}/cell
δ_3	Tumor cell killed by drug	8×10^{-1}/cell/day
σ	Growth rate of tumor	5.14×10^{-1}/day
η_1	CTL death rate	3.42×10^{-10}/cell/day
η_2	Rate of CTL induced tumor death	3.5×10^{-7}/cell/day
τ	Inverse of tumor capacity	1.02×10^{-9}/cell
ξ	Influx of drug	0.23/dosage
μ_1	NK cell death rate	1.0×10^{-7}/cell/day
r	Drug decay rate	9×10^{-1}/cell/day
μ_2	Tumor death rate of NK	6.41×10^{-11}/cell/day
α	Activation rate of CTLs	1.1×10^{-7}/cell/day
δ_1	NK cell killed by drug	6×10^{-1}/cell/day
β	CTL death rate	2.0×10^{-2}/day

Fractional-order models, which incorporate non-integer derivatives, provide a more realistic representation of tumor-immune system interactions by capturing complex dynamics such as memory effects, hereditary processes, and long-range interactions. These models are particularly suited for biological systems like immune responses and tumor growth, where behaviors such as immune evasion, tumor progression, and immune activation are critical. By using methods like HNDM and RPS, fractional-order models can incorporate time delays, feedback mechanisms, and nonlinearities, providing deeper insights into immune exhaustion, checkpoint dynamics, and therapeutic effects, including immunotherapy.

This approach allows for more accurate predictions of tumor evolution, resistance to therapy, and the impact of the tumor micro environment (e.g., oxygen levels, acidity) on immune function. By modeling these dynamics, fractional-order models bridge the gap between mathematical theory and biological reality, aiding the development of better therapeutic strategies and improving predictions of tumor recurrence and immune escape mechanisms. In contrast to traditional integer-order models, fractional-order models are more flexible, capturing the intricacies of real-world tumor-immune system behaviors and providing a deeper understanding of cancer progression and immune responses.

Recent developments in fractional calculus have significantly advanced mathematical modeling. Pasayat and Patra (2023) applied the Shehu transform to solve the fractional-order foam drainage equation, demonstrating its utility in complex

systems [8]. Additionally, their work on fractional sight analysis of the generalized Zakharov-Kuznetsov equation using the Elzaki transform further explored nonlinear wave dynamics [9]. Patra and Pasayat also investigated traveling wave solutions for the generalized fractional-order Fokas equation through the Residual Power Series method, emphasizing the role of fractional methods in nonlinear phenomena [10]. These studies build on foundational texts like Podlubny's work on fractional differential equations [11] and on numerical methods for fractional neutron kinetic and diffusion equations [20]. The theoretical framework provided by Samko, Kilbas, and Marichev also underpins these advancements [6]. Together, these contributions enhance the understanding and application of fractional calculus across various fields.

Mathematical modeling has proven to be an indispensable tool in understanding and predicting complex systems across a variety of domains. For example, a computational stochastic framework has been developed to model the mathematical behavior of severe acute respiratory syndrome coronavirus [3]. Additionally, Bayesian regularization neural networks have been employed to solve language learning systems [15]. The effects of hard water consumption on kidney function have been modeled using radial basis neural networks [1], while fractional-order mathematical models of robots for coronavirus detection have been simulated using Levenberg-Marquardt backpropagation [13]. A novel radial basis neural network was designed for modeling the spread of the Zika virus [17], and hyperbolic tangent sigmoid deep neural networks have been applied to model hepatitis B virus dynamics [16]. Furthermore, scale conjugate gradient neural networks have been used to model the relationship between hard water consumption and kidney function [4]. Gudermannian neural networks, optimized by genetic algorithms, have been applied to ecological models such as three-species food chains and nonlinear smoke dispersal [12, 18]. Finally, artificial neural networks have been used to model the nonlinear dynamics of diseases like influenza [14], further showcasing the versatility of mathematical modeling in both public health and environmental systems.

2. Preliminaries

Let ψ be a non-negative real such that $n-1 \leq \psi < n$ and f be an integrable function in the interval $[b,t]$, $b \geq 0$. Then the definitions of fractional order derivative provided by Riemann-Liouville (R-L) and Caputo for order ψ are presented below.

(i) *R-L derivative:*

$$({}^{RL}D_b^{\psi} f)(t) = \frac{\mathrm{d}^n}{\mathrm{d}t^n} \int_b^t \frac{(t-\hbar)^{n-\psi-1}}{\Gamma(n-\psi)} f(\hbar)\mathrm{d}\hbar, \quad (t > b). \tag{2.1}$$

(ii) *Caputo derivative(CD):*

$$({}^{C}D_b^{\psi} f)(t) = \int_b^t \frac{(t-\hbar)^{n-\psi-1}}{\Gamma(n-\psi)} f^{(n)}(\hbar)\mathrm{d}\hbar, \quad (t > b), \tag{2.2}$$

where, $\Gamma(.)$ represents the gamma function, $f^{(n)}(\hbar) = \frac{\mathrm{d}^n}{\mathrm{d}\hbar^n} f(\hbar)$ and $[\psi]$ denotes the integral part of ψ. The correlation between R-L and CD can be given as below:

Remark 2.1. *For a differentiable function $f(t)$ and $t > b$, we have*

$$({}^{RL}D_b^{\psi} f)(t) = ({}^{C}D_b^{\psi} f)(t) + \sum_{k=0}^{n-1} \frac{(t-b)^{k-\psi}}{\Gamma(k-\psi+1)} f^{(k)}(b),$$

and in specific if $f(t) = (t-b)^{\omega}$, $\omega \notin \{-1, -2, -3, \dots\}$ *and* $t > b$, *we have*

$$ {}^{RL}D_b^{\psi} f(t) = {}^{C}D_b^{\psi} f(t) = D_b^{\psi} f(t) = \frac{\Gamma(\omega+1)}{\Gamma(\omega+1-\psi)}(t-b)^{\omega-\psi}. $$

Remark 2.2. *For* $\psi > 0$, $f(t) = (t-b)^{\omega}$ *with* $\psi - \omega - 1 \in \mathbb{N}_0$ *and* $t > b$,

$$ {}^{RL}D_b^{\psi} f(t) = {}^{C}D_b^{\psi} f(t) = D^{\psi} f(t) = 0. $$

Next, in the context of the Caputo-Farizio derivative, some definitions and findings about Fractional power series(FPS) are provided [5].

Definition 2.1. FPS at $t = t_0$ can be described as below

$$ \sum_{b=0}^{\infty} s_b (t-t_0)^{b\varkappa} = s_0 + s_1(t-t_0)^{\varkappa} + s_2(t-t_0)^{2\varkappa} + \dots; n-1 < \varkappa \leq n,\ n \in N,\ t \leq t_0, $$

where, the coefficients of the power series s_b represent the constants, $b = 0, 1, 2, \dots$.

Theorem 2.1. *Let* g *possess a FPS presentation at* $t = t_0$ *as*

$$ g(t) = \sum_{m=0}^{\infty} c_m (t-t_0)^{m\varkappa};\ t_0 \leq t < t_0 + \rho. $$

If $D_{t_0}^{m\varkappa} f(t), m = 0, 1, 2, \dots$ *are continuous on* $(t_0, t_0+\rho)$, *then it is found that* $c_m = \frac{D_{t_0}^{m\varkappa} f(t_0)}{\Gamma(1+m\varkappa)}$.

Definition 2.2. The NT can be described over the set of the functions

$$ \S = \left\{ \hbar(t) : \exists\ \Upsilon,\ \mathfrak{I}_1,\ \mathfrak{I}_2 > 0,\ |\hbar(t)| < \Upsilon\ e^{\left(\frac{|x|}{\mathfrak{I}_j}\right)},\ if\ \ t \in (-1)^j \times [0, \infty) \right\}, $$

and is given by the following formula

$$ \mathbb{N}\{\hbar(t)\} = \Re(v,u) = \int_0^{\infty} \hbar(ut) e^{-vt} dt, \tag{2.3} $$

where, the operator $\mathbb{N}$ is called the Natural transform operator.

Definition 2.3. The inverse Natural transform of $\Re(v,u)$ is defined as

$$ \mathbb{N}^{-1}\{\Re(v,u)\} = \hbar(t) = \frac{1}{2\pi i} \int_{\gamma-i\infty}^{\gamma+i\infty} \Re(v,u) e^{-vt} dv, \tag{2.4} $$

where the operator $\mathbb{N}^{-1}$ is called the inverse Natural transform operator, v and u are the Natural Transform variables, γ is a real constant and the integral in Eq. (3.3) is taken along $v = \gamma$ in the complex plane $v = x + iy$.

Definition 2.4. NT for n^{th} order derivative can be described as

$$ \mathbb{N}\left[\hbar^n(t)\right] = \Re_n(v,u) = \frac{v^n}{u^n}\Re(v,u) - \sum_{k=0}^{n-1} \frac{v^{n-(k+1)}}{u^{n-k}} \hbar^k(t)\Big|_{t=0}. \tag{2.5} $$

Definition 2.5. NT for arbitrary order $\varkappa$ derivative due to caputo sense is given as

$$\mathbb{N}\left[\mathcal{D}\varkappa\hbar(t)\right] = \frac{v^{\varkappa}}{v^{\varkappa}}\Re(v,u) - \sum_{k=0}^{\varkappa-1}\frac{v^{\varkappa-(k+1)}}{u^{\varkappa-k}}\hbar^{k}(t)\Big|_{t=0}. \tag{2.6}$$

Some basic properties of NT are summerized below

- 1. Linearity : $\mathbb{N}\{m\hbar(t)+n\ell(t)\} = m\mathbb{N}\{\hbar(t)\}+n\mathbb{N}\{\ell(t)\}$.
- 2. Change of scale : If $\mathbb{N}\{\hbar(mt) = \frac{1}{m}\Re(v,u)$.

NT of some fundamental functions

S N	$\hbar(t)$	$\mathbb{N}\{\hbar(t)\} = \Re(v,u)$
1	1	$\frac{1}{v}$
2	t	$\frac{u}{v^2}$
3	$e^a t$	$\frac{1}{v-au}$
5	sinat	$\frac{au}{(v^2+a^2u^2)}$
6	cosat	$\frac{v}{v^2+a^2u^2}$
7	sinhat	$\frac{au}{(v^2-a^2u^2)}$
8	coshat	$\frac{v}{v^2-a^2u^2}$

3. Proposed methodology

3.1. Hybrid Natural Decomposition Method(HNDM)

In this segment, the basic idea of HNDM is given briefly. To explore the concept of HNDM, consider a general nonlinear fractional order differential equation as follows:

$$\mathcal{D}_t^{\varkappa}\Psi + R(\Psi) + S(\Psi) = H, \quad n-1 < \varkappa \leq n, \quad (n \in \mathbb{N}), \tag{3.1}$$

with initial condition

$$\Psi(x,0) = G(x), \tag{3.2}$$

where, $\mathcal{D}_t^{\varkappa}$ denotes the CD,$\Psi = \Psi(x,t)$ is the function to be determined, R and S represent linear and nonlinear differential operators and $H = H(x,t)$ is the source term. Employing NT to Eq. (3.1), we obtain

$$\mathbb{N}[\mathcal{D}_t^{\varkappa}\Psi] = \mathbb{N}[H - \{R(\Psi) + S(\Psi)\}]. \tag{3.3}$$

Implementing the properties of differentiation for NT we get,

$$\frac{v^{\varkappa}}{u^{\varkappa}}\mathbb{N}[\Psi(x,t)] - \frac{v^{\varkappa-1}}{u^{\varkappa}}\Psi(x,0) = \mathbb{N}[H - \{R(\Psi) + S(\Psi)\}]. \tag{3.4}$$

$$\mathbb{N}[\Psi(x,t)] = \frac{G(x)}{v} + \frac{u^{\varkappa}}{v^{\varkappa}}\mathbb{N}[H - \{R(\Psi) + S(\Psi)\}]. \tag{3.5}$$

By employing the initial source (3.2), together with the properties of inverse NT, we get,

$$\Psi(x,t) = G(x) + \mathbb{N}^{(}-1)\left[\frac{u^{\varkappa}}{v^{\varkappa}}\mathbb{N}[H - \{R(\Psi) + S(\Psi)\}]\right]. \tag{3.6}$$

Then we obtain

$$\Psi(x,t) = \mathcal{H}(x,t) - \mathbb{N}^{-1}(\frac{u^{\varkappa}}{v^{\varkappa}}\{\mathbb{N}[R(\Psi(x,t)) + S(\Psi(x,t))]\}), \tag{3.7}$$

where, the term $\mathcal{H}(x,t)$ arises by executing the source term with the given initial condition.

Then the infinite series solution can be written by using HNDM as follows

$$\Psi(x,t) = \sum_{n=0}^{\infty} \Psi_m(x,t). \tag{3.8}$$

To decompose the nonlinear terms, Adomian polynomials are used as

$$Q(\Psi(x,t)) = \sum_{m=0}^{\infty} \mathbb{A}_m, \tag{3.9}$$

where, $\mathbb{A}_m$ represents the Adomian polynomials for $\Psi_0, \Psi_1, \ldots \Psi_m$ and the formula for Adomian polynomial can be given as

$$\mathbb{A}_m = \frac{1}{m!}\frac{d^m}{d\lambda^m}\left[N\left(\sum_{p=0}^{\infty}\lambda^p\Psi_p\right)\right]_{\lambda=0}, m = 0, 1, 2, \ldots. \tag{3.10}$$

Substituting Eq. (3.8) and Eq. (3.9) into Eq. (3.7), we have

$$\sum_{m=0}^{\infty}\Psi_m(x,t) = \mathcal{H}(x,t) - \mathbb{N}^{-1}\left[\frac{u^{\varkappa}}{v^{\varkappa}}\left[\mathbb{N}\left[R\sum_{m=0}^{\infty}(\Psi_m(x,t))\right] + \mathbb{N}\left[\sum_{m=0}^{\infty}\mathbb{A}_m\right]\right]\right]. \tag{3.11}$$

From Eq.(3.11), the solution can be written as

$$\Psi_0(x,t) = \mathcal{H}(x,t).$$

Then we can define the recursive relation for the solution as follows

$$\Psi_{m+1}(x,t) = -\mathbb{N}^{-1}(\frac{u^{\varkappa}}{v^{\varkappa}}[\mathbb{N}[R(\Psi_m(x,t)) + \mathbb{A}_m]]), \tag{3.12}$$

where, $\varkappa \in R$ and $m \geq 0$.

After that, the analytical approximate solution $\Psi(x,t)$ can be written as

$$\Psi(x,t) = \lim_{n\to\infty}\sum_{m=0}^{n}\Psi_m(x,t). \tag{3.13}$$

3.2. Residual Power Series method(RPSM)

To explore the theory of RPSM, let us consider the FPS for $N(t), L(t), T(t)$ and $U(t)$ for $t_0 = 0$ as below

$$\begin{aligned} N(t) &= \sum_{\omega=0}^{\infty} \frac{a_\omega}{\Gamma(1+\omega\varkappa)} t^{\omega\varkappa}, \\ L(t) &= \sum_{\omega=0}^{\infty} \frac{b_\omega}{\Gamma(1+\omega\varkappa)} t^{\omega\varkappa}, \\ T(t) &= \sum_{\omega=0}^{\infty} \frac{c_\omega}{\Gamma(1+\omega\varkappa)} t^{\omega\varkappa}, \\ U(t) &= \sum_{\omega=0}^{\infty} \frac{d_\omega}{\Gamma(1+\omega\varkappa)} t^{\omega\varkappa}, \end{aligned} \tag{3.14}$$

where, $0 \leq t < n$ for some $n > 0$.

Then, the n^{th} truncated series of $N(t), L(t), T(t)$ and $U(t)$ can be defined as follows

$$\begin{aligned} N_n(t) &= \sum_{\omega=0}^{\infty} \frac{a_\omega}{\Gamma(1+\omega\varkappa)} t^{\omega\varkappa}, \\ L_n(t) &= \sum_{\omega=0}^{\infty} \frac{b_\omega}{\Gamma(1+\omega\varkappa)} t^{\omega\varkappa}, \\ T_n(t) &= \sum_{\omega=0}^{\infty} \frac{c_\omega}{\Gamma(1+\omega\varkappa)} t^{\omega\varkappa}, \\ U_n(t) &= \sum_{\omega=0}^{\infty} \frac{d_\omega}{\Gamma(1+\omega\varkappa)} t^{\omega\varkappa}. \end{aligned} \tag{3.15}$$

For $n = 0$, we have $N_0(t) = a_0 = N_0(0) = N_0$, $L_0(t) = b_0 = L_0(0) = L_0$, $T_0(t) = c_0 = T_0(0) = T_0$ and $U_0(t) = d_0 = U_0(0) = U_0$ by using the given initial condition. Then, the n^{th} truncated series in Eq.(3.15) can be defined as follows

$$\begin{aligned} N_n(t) &= N_0 + \sum_{\omega=1}^{n} \frac{a_\omega}{\Gamma(1+\omega\varkappa)} t^{\omega\varkappa}, \\ L_n(t) &= L_0 + \sum_{\omega=1}^{n} \frac{b_\omega}{\Gamma(1+\omega\varkappa)} t^{\omega\varkappa}, \\ T_n(t) &= T_0 + \sum_{\omega=1}^{n} \frac{c_\omega}{\Gamma(1+\omega\varkappa)} t^{\omega\varkappa}, \\ U_n(t) &= U_0 + \sum_{\omega=1}^{n} \frac{d_\omega}{\Gamma(1+\omega\varkappa)} t^{\omega\varkappa}. \end{aligned} \tag{3.16}$$

Now the residual functions for the model Eq.(1.1) can be defined as:

$$\begin{aligned} Res_{N(t)} &=^{C} D_t^{\varkappa} N(t) - (\phi N(1-\lambda N) - \mu_1 NT - \delta_1 UN)), \\ Res_{L(t)} &=^{C} D_t^{\varkappa} L(t) - (\alpha NT - \beta L - \eta_1 LT - \delta_2 UL), \\ Res_{T(t)} &=^{C} D_t^{\varkappa} T(t) - (\sigma T(1-\tau T) - \mu_2 NT - \eta_2 LT - \delta_3 UT), \\ Res_{U(t)} &=^{C} D_t^{\varkappa} U(t) - (\xi - rU). \end{aligned} \tag{3.17}$$

Therefore, the n^{th} residual functions of $S(t), E(t), I(t)$ and $R(t)$ are given as follows

$$\begin{aligned} Res_{N_n(t)} &=^{C} D_t^{\varkappa} N_n(t) - (\phi N(1-\lambda N) - \mu_1 NT - \delta_1 UN), \\ Res_{L_n(t)} &=^{C} D_t^{\varkappa} L_n(t) - (\alpha NT - \beta L - \eta_1 LT - \delta_2 UL), \\ Res_{T_n(t)} &=^{C} D_t^{\varkappa} T_n(t) - (\sigma T(1-\tau T) - \mu_2 NT - \eta_2 LT - \delta_3 UT), \\ Res_{U_n(t)} &=^{C} D_t^{\varkappa} U_n(t) - (\xi - rU). \end{aligned} \tag{3.18}$$

Clearly, $Res_{N(t)} = Res_{L(t)} = Res_{T(t)} = Res_{U(t)} = 0$, for all $t \geq 0$. We know that the derivative of any constant in Caputo-Fabrizio sense is zero. So we can deduce

$$\begin{aligned} {}^{C}D_0^{(k-1)\varkappa} Res_N(0) &=^{C} D_0^{(k-1)\varkappa} Res_{N,k}(0), \\ {}^{C}D_0^{(k-1)\varkappa} Res_L(0) &=^{C} D_0^{(k-1)\varkappa} Res_{L,k}(0), \\ {}^{C}D_0^{(k-1)\varkappa} Res_T(0) &=^{C} D_0^{(k-1)\varkappa} Res_{T,k}(0), \\ {}^{C}D_0^{(k-1)\varkappa} Res_U(0) &=^{C} D_0^{(k-1)\varkappa} Res_{U,k}(0). \end{aligned} \tag{3.19}$$

Then, substitute the n^{th} truncated series of $N(t)$, $L(t)$, $T(t)$ and $U(t)$ into Eq.(3.19) to obtain the co-efficients of $a_\omega, b_\omega, c_\omega$ and d_ω, $\omega = 1, 2, 3, ..., n$ and then apply Caputo fractional operator to the Residual functions. As a result we obtain the equations

$$\begin{aligned} {}^{C}D_0^{(n-1)\varkappa} Res_{N,n}(0) &= 0, \\ {}^{C}D_0^{(n-1)\varkappa} Res_{L,n}(0) &= 0, \\ {}^{C}D_0^{(n-1)\varkappa} Res_{T,n}(0) &= 0, \\ {}^{C}D_0^{(n-1)\varkappa} Res_{U,n}(0) &= 0, \end{aligned} \tag{3.20}$$

for $n = 1, 2, 3, \ldots$

Then by solving the system Eq.(3.20) we obtain the n^{th} residual power series approximation for the values of $a_k, b_k, c_k, d_k, k = 1, 2, 3, \ldots, n$.

4. Applications

4.1. Solution by HNDM

In this segment we apply NT to the fractional order system of differential equation in Caputo sense to acquire the analytical result. Applying NT to model Eq.(1.1)

we obtain

$$\begin{aligned}
&\frac{v^{\varkappa}}{u^{\varkappa}}\mathbb{N}N(t) - \frac{v^{(\varkappa-1)}}{u^{\varkappa}}N_0 = \mathbb{N}\left(\phi N(1-\lambda N) - \mu_1 NT - \delta_1 UN\right),\\
&\frac{v^{\varkappa}}{u^{\varkappa}}\mathbb{N}L(t) - \frac{v^{(\varkappa-1)}}{u^{\varkappa}}L_0 = \mathbb{N}\left(\alpha NT - \beta L - \eta_1 LT - \delta_2 UL\right),\\
&\frac{v^{\varkappa}}{u^{\varkappa}}\mathbb{N}T(t) - \frac{v^{(\varkappa-1)}}{u^{\varkappa}}T_0 = \mathbb{N}\left(\sigma T(1-\tau T) - \mu_2 NT - \eta_2 LT - \delta_3 UT\right),\\
&\frac{v^{\varkappa}}{u^{\varkappa}}\mathbb{N}U(t) - \frac{v^{(\varkappa-1)}}{u^{\varkappa}}U_0 = \mathbb{N}\left(\xi - rU\right).
\end{aligned} \tag{4.1}$$

The nonlinear terms can be decomposed by using the following formula of Adomian polynomials:

$$\mathbb{A}_m = \frac{1}{m!}\frac{d^m}{d\lambda^m}\left[\sum_{p=0}^{n}\lambda^p N_p \sum_{p=0}^{n}\lambda^p T_p\right]_{\lambda=0} \quad , m = 0, 1, 2, \ \ldots \tag{4.2}$$

By using Eq.(4.2), and simultaneously applying inverse NT to Eq.(4.1) we obtain the result as follows

$$\begin{aligned}
&[N_0(t)] = N_0,\ [L_0(t)] = L_0,\ [T_0(t)] = T_0,\ [U_0(t)] = U_0.\\
&[N_1(t)] = \frac{t^{\varkappa}}{\Gamma(1+\varkappa)}\mathbb{N}\left[\phi N_0(1-\lambda N_0) - \mu_1 N_0 T_0 - \delta_1 U_0 N_0\right].\\
&[L_1(t)] = \frac{t^{\varkappa}}{\Gamma(1+\varkappa)}[\alpha N_0 T_0 - \beta L_0 - \eta_1 L_0 T_0 - \delta_2 U_0 L_0].\\
&[T_1(t)] = \frac{t^{\varkappa}}{\Gamma(1+\varkappa)}[\sigma T_0(1-\tau T_0) - \mu_2 N_0 T_0 - \eta_2 L_0 T_0 - \delta_3 U_0 T_0].\\
&[U_1(t)] = \frac{t^{\varkappa}}{\Gamma(1+\varkappa)}[\xi - rU_0].\\
&[N_2(t)] = \frac{t^{2\varkappa}}{\Gamma(1+2\varkappa)}\left[\phi N_1(1-2\lambda N_0) - \mu_1(N_0 T_1 + N_1 t_0) - \delta_1(U_0 N_1 + U_1 N_0)\right].\\
&[L_2(t)] = \frac{t^{2\varkappa}}{\Gamma(1+2\varkappa)}[\alpha(N_1 T_0 + N_0 T_1) - \beta L_1 - \eta_1(L_1 T_0 + L_0 T_1) - \delta_2(U_1 L_0 + U_0 L_1)].\\
&[T_2(t)] = \frac{t^{2\varkappa}}{\Gamma(1+2\varkappa)}[\sigma T_1(1-2\tau T_0) - \mu_2(N_1 T_0 + N_0 T_1) - \eta_2(L_1 T_0 + L_0 T_1)\\
&\qquad - \delta_3(U_1 T_0 + U_0 T_1)].\\
&[U_2(t)] = \frac{t^{2\varkappa}}{\Gamma(1+2\varkappa)}[\xi - rU_1].\\
&\quad\ \vdots
\end{aligned} \tag{4.3}$$

Thus the series solution along with three terms can be written as

$$\begin{aligned} N(t) &= 1\times 10^5 - 682925\frac{t^{\varkappa}}{\Gamma(1+\varkappa)} + 5.9933157835\times 10^6\frac{t^{2\varkappa}}{\Gamma(1+2\varkappa)},\\ L(t) &= 1\times 10^2 - 109397.658\frac{t^{\varkappa}}{\Gamma(1+\varkappa)} + 2.23368\times 10^6\frac{t^{2\varkappa}}{\Gamma(1+2\varkappa)},\\ T(t) &= 1\times 10^7 - 7.4913\times 10^7\frac{t^{\varkappa}}{\Gamma(1+\varkappa)} + 6.3136\times 10^8\frac{t^{2\varkappa}}{\Gamma(1+2\varkappa)},\\ U(t) &= 10 - 8.77\frac{t^{\varkappa}}{\Gamma(1+\varkappa)} + 8.123\frac{t^{2\varkappa}}{\Gamma(1+2\varkappa)}. \end{aligned} \tag{4.4}$$

4.2. Solution by RPS

Here, we explore the RPS method to obtain the numerical result of model Eq.(1.1). Consider the following fractional model for tumor immune cells:

$$\begin{aligned} {}^{C}D_t^{\varkappa}N(t) &= \left(\phi N(1-\lambda N) - \mu_1 NT - \delta_1 UN)\right),\\ {}^{C}D_t^{\varkappa}L(t) &= \left(\alpha NT - \beta L - \eta_1 LT - \delta_2 UL\right),\\ {}^{C}D_t^{\varkappa}T(t) &= \left(\sigma T(1-\tau T) - \mu_2 NT - \eta_2 LT - \delta_3 UT\right),\\ {}^{C}D_t^{\varkappa}U(t) &= \left(\xi - rU\right), \end{aligned} \tag{4.5}$$

subject to $N(0) = 1\times 10^5$, $L(0) = 1\times 10^2$, $T(0) = 1\times 10^7$, $U(0) = 10$ and $0 < \varkappa \leq 1$. By following the steps of RPS as discussed in the previous section we obtain the first truncated power series approximation in the form

$$\begin{aligned} N_0(t) &= 1\times 10^5 + \frac{a_1}{\Gamma(1+\varkappa)}t^{\varkappa},\\ L_0(t) &= 1\times 10^2 + \frac{b_1}{\Gamma(1+\varkappa)}t^{\varkappa},\\ T_0(t) &= 1\times 10^7 + \frac{c_1}{\Gamma(1+\varkappa)}t^{\varkappa},\\ U_0(t) &= 10 + \frac{d_1}{\Gamma(1+\varkappa)}t^{\varkappa}. \end{aligned} \tag{4.6}$$

By applying the values of all the parameters and solving by RPS we obtain the values of a_1, b_1, c_1, and d_1. Hence,

$$\begin{aligned} N_1(t) &= 1\times 10^5 - \frac{682925}{\Gamma(1+\varkappa)}t^{\varkappa},\\ L_1(t) &= 1\times 10^2 + \frac{109397.658}{\Gamma(1+\varkappa)}t^{\varkappa},\\ T_1(t) &= 1\times 10^7 - \frac{7.4913\times 10^7}{\Gamma(1+\varkappa)}t^{\varkappa},\\ U_1(t) &= 10 - \frac{8.77}{\Gamma(1+\varkappa)}t^{\varkappa}. \end{aligned} \tag{4.7}$$

By continuing the same process we obtain the values of a_2, b_2, c_2, and d_2. Thus,

$$\begin{aligned} N_2(t) &= 1 \times 10^5 - \frac{682925}{\Gamma(1+\varkappa)} t^{\varkappa} + \frac{5.993316 \times 10^6}{\Gamma(1+2\varkappa)} t^{2\varkappa}, \\ L_2(t) &= 1 \times 10^2 + \frac{109397.658}{\Gamma(1+\varkappa)} t^{\varkappa} - \frac{2.23368 \times 10^6}{\Gamma(1+2\varkappa)} t^{2\varkappa}, \\ T_2(t) &= 1 \times 10^7 - \frac{7.4913 \times 10^7}{\Gamma(1+\varkappa)} t^{\varkappa} + \frac{6.313637 \times 10^8}{\Gamma(1+2\varkappa)} t^{2\varkappa}, \\ U_2(t) &= 10 - \frac{8.77}{\Gamma(1+\varkappa)} t^{\varkappa} + \frac{7.893}{\Gamma(1+2\varkappa)} t^{2\varkappa}. \end{aligned} \tag{4.8}$$

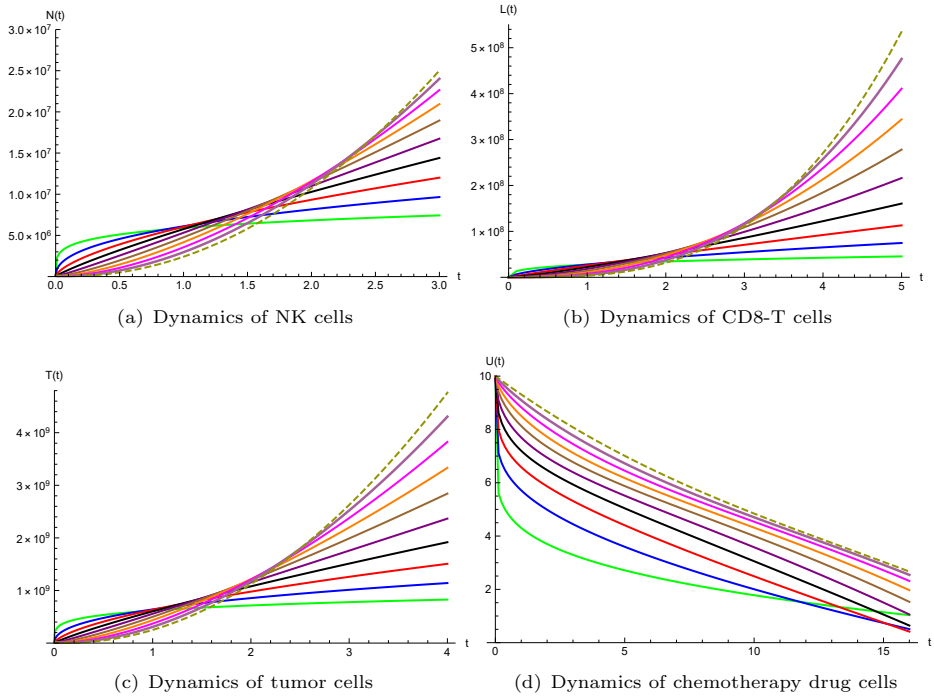

(a) Dynamics of NK cells (b) Dynamics of CD8-T cells

(c) Dynamics of tumor cells (d) Dynamics of chemotherapy drug cells

Figure 1. Plots for the influence of fractional order chemotherapy drugs on cells at the tumor site by using HNDM method

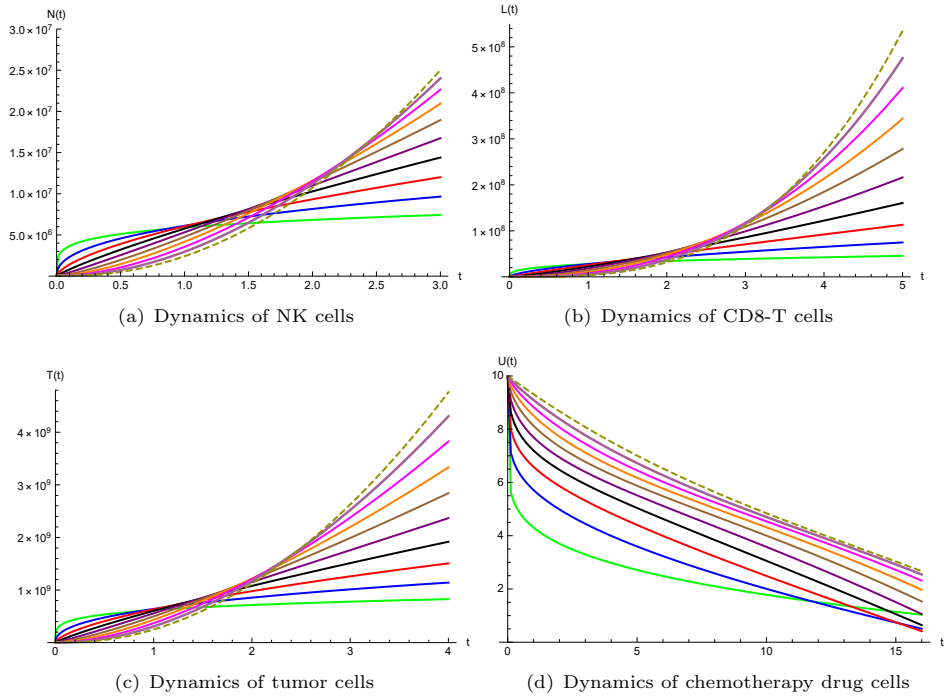

(a) Dynamics of NK cells (b) Dynamics of CD8-T cells

(c) Dynamics of tumor cells (d) Dynamics of chemotherapy drug cells

Figure 2. Plots for the influence of fractional order chemotherapy drugs on cells at the tumor site by using RPS method

5. Discussion

This section provides a detailed overview of the results obtained using the proposed techniques. The experimental outcomes are visually represented in Figs. 1 and 2. Figs. 1a and 2a illustrate the effect of chemotherapy drugs on NK-cell count throughout the treatment period, focusing on the influence of time-fractional orders on the drug's efficacy, as analyzed through HNDM and RPS. The results reveal that the NK-cell count, which initially peaked before drug administration, declined significantly as the treatment continued beyond one month. Similarly, Figs. 1b and 2b show comparable trends in CD8+ T-cells, while Figs. 1c and 2c present a contrasting response in tumor cells under the same chemotherapy regimen. The tumor cell count exhibited an unchecked increase at a constant rate, indicating that improper time-fractional dosage regimens may exacerbate tumor growth. Furthermore, Figs. 1d and 2d highlight a significant reduction in cells carrying chemotherapy drugs over time, particularly at specific intervals. These findings underscore the importance of carefully determining optimal dosage schedules for chemotherapy, as inappropriate time intervals could potentially lead to adverse effects, such as drug resistance and accelerated tumor cell proliferation. Overall, the results depicted in Figs. 1 and 2 emphasize the necessity of tailoring treatment strategies for individual patients to improve therapeutic outcomes. It is noteworthy that, to the best of our knowledge, the solution presented herein is novel and has not been previously established. By leveraging the HNDM and RPS techniques, we are able to attain significantly more accurate results with a reduced computational effort, outperforming the classical

methods documented in the existing literature [7, 22].

6. Conclusion

This study employs the Caputo fractional-order differential operator to model a nonlinear four-dimensional system of differential equations, capturing the intricate dynamics of disease progression through interactions between tumors and immune cells. By incorporating diffusion effects, the proposed system provides a more comprehensive understanding of cellular behavior and disease spread.

The approximate solutions obtained using both analytical and numerical techniques exhibit strong convergence, as confirmed by our Mathematica simulations. A key contribution of this work lies in the effective application of fractional calculus, which not only enhances the accuracy of the model but also enables a more realistic representation of the fractional kill rate of cells using abstract datasets.

Furthermore, a series of detailed graphical simulations illustrate the impact of various dosage regimens on disease progression, reinforcing the theoretical findings and offering valuable insights for future studies. Although this study relies on abstract data, a natural progression of this research will involve validating the model with real-world clinical data, paving the way for more precise and personalized therapeutic strategies in oncology.

Ethical Standard

The authors declares that this research complies with ethical guidelines. This research does not involve either human participants or animals.

Authors contribution

Tapasi Pasayat : conceptualization of the study, original draft, mathematical programming by using software Mathematica. Ashrita Patra: Writing review and editing.

Conflict of Interest

The authors declare that they have no conflicts of interest regrading the publication of this paper.

Availability of Data

Not Applicable.

References

[1] A. A. Alderremy, D. Hernández-Castañeda, J. F. Gómez-Aguilar et al., *Radial basis neural network for the hard water consumption with kidney model*, International Journal of Geometric Methods in Modern Physics, 0, 0(0), 2550090.

[2] S. Alshammari, M. Alshammari, M. Alabedalhadi et al., *Numerical investigation of a fractional model of a tumor-immune surveillance via caputo operator*, Alexandria Engineering Journal, 2024, 86, 525–536.

[3] A. Asghar, M. Hassan, Z. Sabir et al., *A design of computational stochastic framework for the mathematical severe acute respiratory syndrome coronavirus model*, Biomedical Signal Processing and Control, 2025, 100, 107049.

[4] A. Asghar, Z. Sabir and M. Hassan, *A scale conjugate gradient neural network for the hard water consumption using the kidney function*, The European Physical Journal Plus, 2024, 139.

[5] S. Hasan, A. Alzoubi, A. Freihat et al., *Solution of fractional sir epidemic model using residual power series method*, Applied Mathematics and Information Sciences, 2019, 13, 153–161.

[6] A. A. Kilbas, O. I. Marichev and S. G. Samko, *Fractional integrals and derivatives (theory and applications)*, 1993.

[7] O. Morufu Oyedunsi and A. Adedapo Ismaila, *A space-time caputo fractional order and modified homotopy perturbation method for evaluating the pathological response of tumor-immune cells*, Healthcare Analytics, 2024, 5, 100325.

[8] T. Pasayat and A. Patra, *Solution of fractional order foam drainage equation using shehu transform*, in *Advances in Mathematical Modelling, Applied Analysis and Computation* (Edited by J. Singh, G. A. Anastassiou, D. Baleanu and D. Kumar), Springer Nature Switzerland, Cham, 2023, 317–331.

[9] T. Pasayat, A. Patra and M. Sahoo, *Fractional sight analysis of generalized perturbed zakharov–kuznetsov equation using elzaki transform*, Japan Journal of Industrial and Applied Mathematics, 2023, 41.

[10] A. Patra and T. Pasayat, *Travelling wave solution for generalised (4+1) dimensional fractional order fokas equation using residual power series method*, International Journal of Theoretical Physics, 2025, 64.

[11] I. Podlubny, *Fractional differential equations: Academic press, new york*, Academic Press, New York, 1999.

[12] Z. Sabir, M. Ali and R. Sadat, *Gudermannian neural networks using the optimization procedures of genetic algorithm and active set approach for the three-species food chain nonlinear model*, Journal of Ambient Intelligence and Humanized Computing, 2022, 14, 8913–8922.

[13] Z. Sabir, M. Ali and R. Sadat, *Simulation of fractional order mathematical model of robots for detection of coronavirus using levenberg-marquardt backpropagation neural network*, Neural Computing and Applications, 2024, 36, 22417–22428.

[14] Z. Sabir, T. Botmart, M. A. Z. Raja et al., *Artificial neural network scheme to solve the nonlinear influenza disease model*, Biomedical Signal Processing and Control, 2022, 75, 103594.

[15] Z. Sabir, S. Khansa, G. Baltaji and T. Saeed, *A bayesian regularization neural network procedure to solve the language learning system*, Knowledge-Based Systems, 2025, 310, 112997.

[16] Z. Sabir, I. Kotob, L. Sheikh and T. Saeed, *A novel computational approach based hyperbolic tangent sigmoid deep neural network for the hepatitis b virus*

model, International Journal of Geometric Methods in Modern Physics, 2024, 22.

[17] Z. Sabir, T. B. Rada, Z. Kassem et al., *A novel radial basis neural network for the zika virus spreading model*, Computational Biology and Chemistry, 2024, 112, 108162.

[18] Z. Sabir, M. A. Z. Raja, A. Alnahdi et al., *Numerical investigations of the nonlinear smoke model using the gudermannian neural networks*, Mathematical Biosciences and Engineering, 2021, 19, 351–370.

[19] Z. Sabir and M. Umar, *Levenberg-marquardt backpropagation neural network procedures for the consumption of hard water-based kidney function*, International Journal of Mathematics and Computer in Engineering, 2023, 1.

[20] S. Saha Ray and A. Patra, *Application of homotopy analysis method and adomian decomposition method for the solution of neutron diffusion equation in the hemisphere and cylindrical reactors*, J. Nucl. Eng. Technol., 2011, 1, 1–14.

[21] R. Singh, J. Mishra and V. Gupta, *The dynamical analysis of a tumor growth model under the effect of fractal fractional caputo-fabrizio derivative*, International Journal of Mathematics and Computer in Engineering, 2023, 1.

[22] G. Song, G. Liang, T. Tian and X. Zhang, *Mathematical modeling and analysis of tumor chemotherapy*, Symmetry, 2022, 14, 704.

[23] S. Venkatesan, C. Swanton, T. B. S. and J. F. Costello, *Treatment-induced mutagenesis and selective pressures sculpt cancer evolution*, Cold Spring Harbor perspectives in medicine, 2017.